Quantitation of endogenous metabolites in mouse tumors using mass-spectrometry imaging

SWALES, John, DEXTER, Alex, HAMM, Gregory, NILSSON, Anna, STRITTMATTER, Nicole, MICHOPOULOS, Filippos, HARDY, Christopher, MORENTIN-GUTIERREZ, Pablo, MELLOR, Martine, ANDREN, Per E., CLENCH, Malcolm <http://orcid.org/0000-0002-0798-831X>, BUNCH, Josephine, CRITCHLOW, Susan E. and GOODWIN, Richard J. A.

Published version

SWALES, John, DEXTER, Alex, HAMM, Gregory, NILSSON, Anna, STRITTMATTER, Nicole, MICHOPOULOS, Filippos, HARDY, Christopher, MORENTIN-GUTIERREZ, Pablo, MELLOR, Martine, ANDREN, Per E., CLENCH, Malcolm, BUNCH, Josephine, CRITCHLOW, Susan E. and GOODWIN, Richard J. A. (2018). Quantitation of endogenous metabolites in mouse tumors using mass-spectrometry imaging. Analytical Chemistry, 90 (10), 6051-6058.

Copyright and re-use policy

Quantitation of endogenous amino acids in mouse tumors using mass spectrometry imaging

John G. Swales[1, 3], Alex Dexter[4], Gregory Hamm[1], Anna Nilsson[5], Nicole Strittmatter[1], Filippos N. Michopoulos[2], Christopher Hardy[1], Pablo Morentin-Gutierrez[2], Martine Mellor[2], Susanne Critchlow[2], Per Andren[5], Josephine Bunch[4], Malcolm R. Clench[3], Richard J.A. Goodwin[1]

[1] Pathology, Drug Safety & Metabolism, IMED Biotech Unit, AstraZeneca, Cambridge, UK
[2] Oncology Bioscience, IMED Biotech Unit, AstraZeneca, Cambridge, UK
[3] Centre for Mass Spectrometry Imaging, Biomolecular Research Centre, Sheffield Hallam University, Sheffield, UK
[4] National Centre of Excellence in Mass Spectrometry Imaging (NiCE-MSI), National Physical Laboratory, Teddington, TW11 0LW, United Kingdom
[5] Biomolecular Imaging and Proteomics, National Center for MSI, Uppsala University, Sweden

Short title: Quantitation of enodgenous small molecules by MALDI MSI

Keywords: MALDI, MSI, Imaging, Quantitation, Lactate, Glutamate

Corresponding author:

Email: john.swales@astrazeneca.com
Address: AstraZeneca, Darwin Building, Cambridge Science Park, Milton Road, Cambridge, Cambridgeshire, CB4 0WG, UK
Tel. +44(0)1223 223417

Abstract

Mass spectrometry imaging (MSI) is increasingly being used as a label free method of evaluating the distribution of drugs and endogenous compounds in tissues. The technology has been welcomed by drug researchers eager to perform drug distribution studies at an earlier stage in the discovery timeline. The technology however is not limited to drug distribution studies but can also be used to detect a wide range of chemical species rendering it applicable to both pharmacokinetic and pharmacodynamic endpoints. Traditionally MSI has been used in a qualitative capacity, however it is increasingly being used for quantitative assessments of drug levels in tissue sections.

Here we report quantitative mass spectrometry imaging (qMSI) methodology for the analysis of endogenous amino acids (lactate and glutamate) in mouse tumor models. We describe pre-analysis stabilization methods aimed at improving quantitative assessment of endogenous small molecules. Additionally, we apply qMSI methodology to monitor lactate modulation in tumors after dosing animals with a proprietary drug (AZx) known to effect energy metabolism in cancer cells. Finally, we use regio-specific qMSI to identify a tumor model that has low lactate heterogeneity in an effort to decrease inter tumor variability and enable accurate measurement of lactate modulation in pre-clinical efficacy studies.

Introduction

Oncology is a growing research area in pharmaceutical R&D. The complex nature of cancer has prompted research into many potentially therapeutic pathways targeting changes in cancer cell growth, division, proliforation and death, making the space highly competitive and congested. In the search for ever more novel approaches in the fight against cancer researchers have now begun to focus on ways to make the body's own immune system specifically target cancer cells, an area known as immuno-oncology.

A common difference between tumor cells and normally differentiated cells is a change in cellular metabolism. Otto Warburg documented the classic metabolic shift of cancer cells to aerobic glycolysis, higher energy production and increased lactate concentration[1]. More recently Vander Heiden et al. have hypothesized that adaptations to the metabolic pathways in tumor cells are an aide to cellular proliferation, facilitating uptake and incorporation of nutrients into the constituents needed for the generation of new cells[2]. The list of pathways affected by cellular disease state is wide and varied and as such has become the focus of pharmaceutical companies wishing to find new pharmacological targets and ultimately improve the living standards of cancer patients.

Metabolic features of the Warburg effect are a hallmark of cancer, where most tumors rely on glucose and glutamine catabolism to produce ATP and the building blocks necessary to sustain rapid cell growth[3]. The balance of nutrients and oxygen within the tumor microenvironment controls immune cell function. Glucose and amino acid consumption by tumor cells can outpace that of infiltrating immune cells, specifically depriving them of nutrients to fuel their effector function. Poorly perfused tumor regions drive hypoxia response programs in tumor cells, macrophages, and T cells. Increased HIF-1a activity in response to hypoxia or other mechanisms promotes glycolysis and increases concentrations of suppressive metabolites and acidification of the local environment. As a by-product of glycolysis, lactate concentration increases, which is co-ordinately utilized by tumor cells to fuel their metabolism, promote macrophage polarization, and directly suppresses T cell function[4]. Kreutz and colleagues (Brand et al., 2016) reported a novel mechanism whereby lactic acid produced by highly glycolytic tumors overcomes immune surveillance, by impairing activation of infiltrating cytotoxic CD8+ T and NK cells[5].

Developing therapeutic approaches to modify T cells to utilize lactate as an energy and biomolecule source, similar to the pathways operating in some tumor cells, or reducing the

levels of lactate in the micro-environment may provide means to overcome this hurdle for tumor immunity.

Analytical methodologies that enable quantitative evaluation of tumor lactate levels in the tumor microenvironment are critical when developing potential new treatments. Furthermore, given the complex and heterogenic tumor architecture, spatial information of tumor lactate levels can provide valuable information to better understand both the endogenous distribution of tumor lactate and also the effects on endogenous levels after drug dosing in animal model efficacy testing. This understanding can then enable reliable pharmacokinetic-pharmacodynamic (PK-PD) understanding of the modulation of tumor lactate levels and how they correlate with overall effects on tumor growth.

Drug discovery is a lengthy, costly and competitive business. Potential new drugs can take more than ten years to reach commercialization, at a cost of billions of dollars. Furthermore, attrition rates during the later stages of development increase the already high risk factors involved with taking a new compound into the clinic[6]. Pharmaceutical companies have gone to great lengths to decrease these high failure rates, minimising risk in an effort to maximize reward and bring new medicines to the market[7]. Poor efficacy and toxicity are the main reasons for high attrition rates within research and development (R&D)[8]. The industry has addressed this problem by adopting a strategy of early, accelerated compound optimisation with parallel generation of physicochemical and pharmacokinetic properties to design safer and more efficacious drug candidates that maximize therapeutic index whilst minimising any risk of toxicity[9].

Bioanalytical techniques such as LC-MS have kept pace with the need for higher throughput[10] but are limited in value when trying to assess a drug's distribution *in vivo*. Traditionally drug distribution studies were performed during the later stages of development using radiolabelled compounds in low throughput techniques such as qWBA[11] or homogenization[12] studies using

LC-MS with long liquid chromatography gradients. Mass spectrometry imaging (MSI) is a term given to a group of label free, multiplex analytical techniques that can essentially map the molecular distribution of endogenous compounds, drugs[13], lipids[14], proteins[15], peptides[16] and drug delivery systems[17] in biological tissues. MSI techniques are all based on different mass spectrometry surface sampling ion sources of which matrix assisted laser desorption ionization mass spectrometry imaging (MALDI-MSI)[18] has arguably the most widespread use within the pharmaceutical industry. MALDI-MSI is being rapidly joined by other MSI techniques such as desorption electrospray ionization mass spectrometry imaging (DESI-MSI)[19] and liquid extraction surface analysis mass spectrometry imaging (LESA-MSI)[20] that bring complementary properties such as an expanded chemical scope and increased sensitivity, usually at the expense of decreased spatial resolution. Essentially, each technique rasters or continuously scans across tissue sections acquiring a constant full mass spectrum at each pixel or coordinate, each mass signal within the spectrum is assigned an intensity that can then be color coded into a heat map image describing the relative abundance of an analyte within the tissue.

Whilst not replacing traditional bioanalysis, MSI is increasingly being used alongside these techniques providing timely and cost effective insights into the deposition and fate of new chemical entities[21]. The application of the technique has been expanded further to encompass endogenous compound changes as markers for drug induced efficacy[22] or toxicity[23].

Applications of MSI within the drug discovery industry are well documented[24]. It has increasingly been used to provide molecular distribution information at an early stage of the drug development pipeline. Several groups have reported successful imaging of low mass endogenous metabolites in tumors[25]. Data has largely been qualitative in nature but in order to expand the applicability of MALDI-MSI into pharmacodynamic testing of compound

efficacy, quantitative mass spectrometry imaging (qMSI) methods are needed that can spatially resolve regions of high abundance in what is often complex tumor architecture. Here we present a mass spectrometry imaging methodology for the absolute quantitation of two key endogenous metabolites involved in tumor cell energy production (glycolysis and the TCA cycle), lactate and glutamate. The techniques developed were used to screen several mouse tumor models to identify a suitable phenotype to reliably monitor lactate changes post drug administration in efficacy studies. We also present regiospecific quantitation post spectral segmentation to highlight the heterogeneity of each tumor model.

Methods

Materials and reagents

Analytical grade acetonitrile, methanol and formic acid were obtained from Fisher Scientific (Loughborough, Leicestershire, UK). 2-methylbutane, gelatin, lactate-^{13}C3, lactate ^{13}C1, Glutamate-D3, 1, 5-diaminonaphthalene and 9-aminoacridine were purchased from Sigma-Aldrich (Poole, Dorset, UK). Test compound for the efficacy study was obtained in-house from AstraZeneca compound management group (Macclesfield, Cheshire, UK). Lactate-^{13}C1 and Glutamate-D5 were purchased from QMX Laboratories (Thaxted, Essex, UK).

Amino acid stability in rat kidney sections

Duplicate control kidney sections (10µm) were cut and mounted onto glass microscope slides over a 24h time-course (0, 0.5, 18, 21 & 24h). Sections were stored at one of three different conditions between time-points; (1) left in the cryostat thaw mounted at -16ºC, (2) thaw mounted, dessicated in N_2, vacuum packed and stored at ambient temperature, or (3) thaw mounted, dessicated in N_2, vacuum packed and stored at -80ºC. A ‘fresh’ kidney section was

mounted on each slide prior to analysis by desorption electrospray mass spectrometry imaging.

Animals studies

All animal studies were conducted in accordance with UK Home Office legislation, the Animal Scientific Procedures Act 1986, and the AstraZeneca Global Bioethics policy. All experimental work is outlined in home office license 40/8894, which has gone through the AstraZeneca Ethical Review Process.

Initial proof of priciple study (AZx)

AZx was dosed at 3 dose levels (3, 30 and 100 mg/kg) to athymic nude mice from a NCI-H358 tumor model over an 8 day period. Five animals from each dose level were sacrificed at 0.5, 2, 6 and 24 h post dose. Five time-matched vehicle dosed animals at each dose level were also euthanized to act as a direct comparison. All tumors were resected at necropsy and snap frozen in dry ice chilled 2-methyl butane. The tumors were stored at -80°C prior to cryo-sectioning and subsequent analysis.

Mouse models (Screening)

Four different female athymic nude mice tumor models were screened for lactate and glutamate concentration and distribution. The four models tested were NCI-H358 (a human xenograft model grown in nude mice), MC38, B16.F10.AP3 and a MC38 Variant (all syngeneic mouse tumor models)

Tissue Embedding

Tissue embedding methodology can be found in the supplementary information.

Sectioning

Details of the methodology used in cryosectioning the tissues used in this study can be found in the supplementary information.

DESI mass spectrometry imaging

Details of the DESI-MSI method used in the stability experiments can be found in the supplementary information.

Lactate calibration standard preparation

Three stock solutions of Sodium L-lactate-^{13}C3 solution (Sigma-Aldrich, 485926-500MG) were prepared daily as needed at concentrations of 500, 5000 and 50000 µM in 50/50 v/v Methanol/Water. A sample of blank 50/50 v/v methanol/water was also retained.

Calibration spots for quantitation were added to control tissue sections (on each day of analysis) using a Preddator robotic liquid handler (Redd and Whyte, London, UK), at amounts equal to 0, 10, 25, 50, 100, 250 and 500 ng of lactate on-tissue. The liquid handler dispensed 50 nL droplets of the standards and over spotting in a total of 4 cycles to reach the required on-tissue amounts of the analyte. Spots were allowed to dry at room temperature prior to matrix addition.

Glutamate calibration standard preparation

Stock solutions of D3-glutamate and D5-glutamate were prepared daily at 100 mM in 0.1 M HCl. D5-glutamate standards were prepared by dilution in 50 % EtOH to concentrations of 2 mM, 0.67 mm, 0.22 mM, 0.074 mM, and 0.025 mM. 0.1 µl of the standards and a blank sample (50% EtOH) were manually applied to control tissue. D5-glutamate was used as an

internal standard. 50 µl of the stock solution was added to 5.95 ml of 50% MeOH and sprayed onto the tissue before matrix application application using a TM-sprayer (HTX technologies, Chapel Hill, NC, USA) with the following parameters; 6 passes at 90°C using a flow 50% methanol/water *v/v* at a flow rate of 0.07 mL/min and nebulized with nitrogen at 6 psi.

MALDI Matrix Application

Details of automated matrix application methods for lactate and glutamate analysis can be found in supplementary information.

MALDI Quantative Mass Spectrometry Imaging (qMSI)

MALDI-MSI experiments were carried out in negative reflectron mode over a mass range of *m/z* 60 to 1000 using a MALDI RapiFlex tissuetyper (lactate) or a UltrafleXtreme (glutamate) MALDI-TOF/TOF MS (Bruker Daltonics, Bremen, Germany) equipped with a 10kHz Smartbeam 3D™ and a 2 kHz, smartbeam-II™ Nd:YAG laser respectively. Data was collected on the RapiFlex was at a spatial resolution of 50 µm, summing up 500 laser shots/raster position. Data collection on the UltrafleXtreme was at a spatial resolution of 80 µm, summing up 300 laser shots /raster position.

FlexImaging 5.0 (Bruker Daltonics, Bremen, Germany) software was used for initial data analysis. Normalization, molecular image extraction and regions of interest for lactate quantitation were defined in SCiLS Lab 2017b (Supplier ?) software typically using mass selection window of ± 0.05 Da. Glutamate quantitation was performed using msIQuant software[26]. Endogenous lactate, lactate ^{13}C1 (for normalization) lactate ^{13}C3 were detected at m/z 89.1, 90.1 and 92.1 respectively.

Spectral Clustering Analysis

Data were imported into Matlab (version R2017a and statistics toolbox, The Math-Works, Inc., Natick, MA, USA) using SpectralAnalysis version 1.01[27]. Briefly, a mean spectrum was generated for each dataset, which was peak picked using the SpectralAnalysis gradient peak picking. These peaks were then extracted into a datacube by integrating under the area for each peak. Data were then normalised to the ^{13}C lactate or glutamate peak (nominally m/z 90.028 and 147.048). These lactate and glutamate concentrations were then quantified to the calibration curves generated from spots applied to a separate tissue section. Clustering was then performed on each of the individual tissue sections using k-means clustering with k = 2-5 (k = 4 shown), using the cosine distance metric[28]. Boxplots of lactate and glutamate concentration were generated using the Matlab function "boxplot" where the central line shows the median concentration, the box represents the 25-75% interquartile range of the data and the whiskers are one additional interquartile range above and below these. Any points outside this range are considered outliers marked by red crosses.

Homogenization and Quantitation of Lactate Levels by LC-MS

Details of the homogenization and LC-MS method can be found in the supplementary information.

Results and Discussion

Endogenous Amino Acid Stability Experiment

Previous in-house experience of endogenous metabolite analysis using DESI-MSI had suggested that degradation of endogenous lactate within rat kidney tissue during sample preparation (data not reported) was possible. This *ex-vivo* change in endogenous small molecule levels was found to be related to the amount of time the tissues spent in the -20°C

environment of the cryomicrotome during the sectioning process and appeared to stabilize during analysis when the sample is removed from the freezer and effectively kept in a desiccated nitrogen rich environment on the DESI stage. Prior to embarking on a quantitative study of lactate and glutamate concentrations in different tumor models it was thus necessary to establish a protocol to stabilize or make sure any degradation of the endogenous compounds within the tissues was as uniform as possible. Kidney sections were taken over a time course spanning 24h in total, the resulting sections were stored between time-points in one of three different conditions; (1) left in the cryostat thaw mounted at -16ºC, (2) thaw mounted, desiccated in N_2, vacuum packed and stored at room temperature, or (3) thaw mounted, desiccated in N_2, vacuum packed and stored at -80ºC. Sections from each time-point were analyzed in duplicate using DESI-MSI, a 'fresh' section was added to each slide immediately before analysis to give a baseline relative abundance of lactate (lac), aspartate (asp), glutamate (glu) or glutamine (glut) for comparison. DESI-MSI images and relative abundances derived from the analysis can be seen in figure 1. The images were spectrally segmented to separate the kidney cortex from the medullary region as the distribution of the amino acids was different in the two areas. As suspected, sections stored under conditions (1) exhibited a degradation of the signal corresponding to the four amino acids in the cortex over time. Lac, asp and glut response in the medulla of the kidney initially dropped but then remained stable at subsequent time-points. Asp levels trended in the opposite direction under the same conditions showing higher abundance in the medulla the longer the sections were stored. Sections stored under conditions (2) decreasing lac levels over the storage time in the renal cortex with a more stable response in the medulla over time. Glu and glut degradation in the cortex and medulla did stabilize under conditions (2), asp again showed a trend towards higher relative abundance over time in both tissue regions. Sections stored under conditions (3), indicated lac levels were more stable than those observed in (1) and (2) in both the cortex

and medulla giving a δ value of 3913 & 8740 respectively, versus δ 28971 & 11691 in the cortex of kidneys stored in (1) and (2) and 42713 and 12094 in the medullary regions. Glu, Asp and glut levels were also found to be more stable under conditions (3) with corresponding improvements in δ values. These results highlighted the need for -80ºC storage, even over a short period of time.

Interpreting the results further, it was clear that immediate desiccation post sectioning followed by vacuum packing and storage at -80ºC was needed to minimize the degradation of the endogenous metabolites in the tissue, however even with this safeguard, instability could still occur as multiple sections were cut one at a time onto the same microscope slide within the cryostat. To minimize the amount of time sections were kept in the cryostat chamber it was decided to embed multiple tissues in gelatin and section them all in a single cut of the microtome blade. This significantly reduces the amount of time the sections spend at temperatures higher than -20°C, with the added bonus of reduced sample preparation time. The embed, thaw mount, desiccate, vaccum pack and store at -80°C protocol was thus adopted for all subsequent analysis.

Initial proof of principle

In order to test the hypothesis that it was possible to quantify and map the spatial distribution of lactate in tumor tissue using qMSI, an initial study was performed in a NCI-H358 human xenograft mouse tumor model. Animals were treated with a proprietary drug (AZx) that is known to induce changes in tumor metabolism. Lactate distribution and concentration levels from tumors treated with AZx were compared to vehicle dosed control animals. Although DESI-MSI had been used in the initial stability experiments it was decided to proceed with a more validated quantitative imaging platform, MALDI-qMSI was thus used to map and quantify the lactate distribution within the tumor tissue. Due to the unavailability of a second

stable-labelled version of lactate this analysis was performed with normalization to total ion current. The results from the analysis (Figure 2) showed that lactate changes could be observed in the tumor tissue after exposure with AZx. The analytical method performed well giving a linear response (R^2 = 0.997) across the calibration range (Figure 2b), stable isotope-labelled (^{13}C3-lactate) calibration spots can be seen in blue in figure 2a. The dynamic range of the calibration line covered the lactate concentrations measured in the tumor tissue (170.0 – 3525.6 µM). Lactate modulation was observed at 2 hours post dose (figure 2c, 100 mg/kg data shown as representative) which corresponded with the maximum concentration (Cmax) of orally administered AZx suggesting the pharmacodynamic response was linked to the pharmacokinetics of the drug. Lactate concentrations at 30 mins, 6 and 24 hrs were similar to those in the vehicle dosed animals. Mean intra-tumoral lactate levels in the control animals at each timepoint was 490.6 – 2464.0 µM giving a corresponding variation of 26.0 – 49.3% CV (n=4 animals at each timepoint) indicating a high level of variation between the vehicle dosed animals. Using the multiplex nature of MALDI-MSI it was possible to simultaneously map the distribution of glutamate (figure 2a) and the drug (data not shown) along with the lactate within the same tumors. Glutamate was distributed throughout the tumors, this was in stark contrast to lactate which was much more heterogeneously distributed and localized into the necrotic or pre-necrotic regions (identified using H&E staining) of the tissue. Glutamate levels in these lactate rich regions were much lower than those observed in the surrounding tissue giving a visual representation of the 'Warburg effect'.

Tumor model screening

The heterogeneous lactate distribution in the NCI-H358 tumor model used in the initial study had been shown to lead to high inter-tumor variation in lactate levels. This could be due to several factors including the tumor model itself and the duration at which the tumors are

allowed to mature. High inter-animal variation decreases the likelihood of detecting subtle differences in endogenous amino acid levels in the dosed animals compared to vehicle treated animals, this could be the reason that no lactate modulation was observed in the early and late timepoints of the initial study. A tumor model that exhibits a more homogeneous lactate distribution would be highly desirable and should reduce the inter-tumor variability giving a more robust model to move forward into efficacy testing and ultimately build a reliable PK/PD model. Several different tumor models were selected for lactate screening. An NCI-H358 model, differentiated from the initial study by allowing the tumor to grow for less time and minimize the chance of necrosis, an MC38 model, a B16.F10.AP3 model and a MC38 variant model were all screened using MALDI-MSI for both lactate and glutamate quantitation and distribution (adjacent sections). Models were analysed in different analytical batches (n=4 for each amino acid), the analytical method performed reliably throughout the analysis, calibration lines gave a consistent linear response (R^2 = 0.9960 – 0.9978) with a gradient range of 0.0041 – 0.0098 and a intercept range of 0.0249 – 0.2649. Ion images are shown in Figure 3a. Tumors from the MC38 and B16.F10.AP3 models showed heterogeneous lactate distribution throughout the tumor tissue with little or no co-localization with glutamate. The MC38 tissue in particular had large areas of necrosis (confirmed by H&E), B16.F10.AP3 tumors were less necrotic but lactate and glutamate distribution was very localized and ‘patchy’ throughout the tissue. The NCI-H358 and MC38 variant tumors had more evenly distributed lactate and glutamate even in areas that were confirmed to be necrotic by H&E staining.

Lactate and glutamate concentrations across each of the tissue sections were largely in the same range between the different models fluctuating between 81.7 – 2504.0 µM for lactate and 10955.0 – 78187.0 µM for glutamate.

Regio-specific qMSI

Spectral clustering was performed on each of the individual tissue sections from each model using k-means clustering with k = 2-5 (k = 4 shown), using the cosine distance metric. This analysis allowed regio-specific pixel by pixel quantitation of the lactate and glutamate levels to be calculated, this is represented graphically in the box plots in figure 4. From the boxplots of lactate and glutamate concentration in each region of each tissue, the lactate concentration was much more heterogeneous in the B15.F10 and MC38 models as seen by the large boxes, whiskers and many outliers. In comparison, the MC38 variant and NCI-H358 tumours have more homogeneously distributed lactate concentration (smaller boxes) with the MC38 variant displaying lower median inter-tumor lactate concentration variability. The glutamate concentration in all tissue models is overall less heterogeneous than the lactate concentration, with the different models containing similar levels of heterogeneity as seen by similar spreads of the data in the boxplots.

The objective of the screening exercise was to identify a tumor model that had greater lactate homogeneity, lower lactate variability and fewer areas of necrosis. The MC38 variant model was selected as the analysis had shown this exhibited the most favorable properties of the four models tested. Subsequently, the MC38 variant model has allowed further efficacy studies to be performed. The more homogeneous lactate distribution and lower variability in the MC38 variant model highlighted by the qMSI analysis has provided the confidence to analyze later studies using non-spatially resolved LC-MS with tissue homogenization. Initial data from the first study suggests that lactate levels within the control tumors measured by LC-MS resulted in a mean concentration of 473.4 µM ± 21.6% based on n=9 control tumors from the MC38 variant model. Comparison of the vehicle dosed tumor lactate data with lactate data from tumors taken from animals dosed with an AZ project compound yielded statistically

significant lactate modulation. The tumor model is now being effectively used to develop a PK/PD relationship to optimize efficacy in subsequent project compounds.

Conclusion

Early confirmation of drug efficacy in humans is of great value to drug discovery projects. Cellular or enzymatic assays can be used to determine compound potency but are rarely a substitute for *in vivo* experiments in syngeneic preclinical animal models. Determination of efficacy endpoints that are directly related to the target pathway in the form of endogenous metabolite differences in diseased human tissue is a gold standard. Thiscan however be misleading in complex tissue environments such as tumor tissue due to localization of the metabolites into different tissue compartments within the tumor.

Here we have established sample pre-treatment protocols that minimize the degradation of endogenous amino acids within sectioned tissue, all tissues are handled in a standardized way and stored under the same conditions to ensure any degradation that does occur is uniform across all sections in the same experiment.

We have demonstrated that the spatial resolution MSI can offer can be successfully used to assess the distribution of endogenous metabolites within different tumor models. We have also shown that MALDI-MSI can be used as a quantitative technique to measure the absolute concentration of these metabolites *in situ*, furthermore, we have shown how spectral clustering can be used to generate regio-specific concentration data within the tumor sections to give a more empirical illustration of tumor heterogeneity.

Quantitative MSI methods such as those reported in this work can be expanded in the future. The multiplex nature of qMSI methods could allow simultaneous quantitation of several endogenous compounds in the same tissue section, it can also be used to encompase different endogenous compound classes such as lipids, peptides and proteins that can modulate with

disease state and give evidence of target engagement or drug efficacy in many other potential therapeutic targets.

Author contributions

PMG, MM and SC designed all in vivo studies and contributed to the manuscript. FNM developed the homogenization methodology and produced all LC-MS data.
JGS, GH, AN and CH developed the quantitative MSI methodology and performed all of the imaging experiments. JGS and NS designed and performed the stability experiments and DESI-MSI analysis. AD performed additional data processing. RJAG, MRC, PA and JB contributed to the production of the manuscript, general methodology discussions and support. JGS wrote the manuscript with feedback from all authors.

Conflicts of interest

The authors do not know of any competing financial interests impacting the generation of this work.

Funding

All studies were funded solely by AstraZeneca PLC.

References

1. Warburg, O., On the origin of cancer. *Science* **1956,** *123* (3191), 309-314.
2. Vander Heiden, M. G.; Cantley, L. C.; Thompson, C. B., Understanding the Warburg effect: the metabolic requirements of cell proliferation. *science* **2009,** *324* (5930), 1029-1033.
3. Scott, Kristen E. N.; Cleveland, John L., Lactate Wreaks Havoc on Tumor-Infiltrating T and NK Cells. *Cell Metabolism* **2016,** *24* (5), 649-650.
4. Buck, M. D.; Sowell, R. T.; Kaech, S. M.; Pearce, E. L., Metabolic Instruction of Immunity. *Cell* **2017,** *169* (4), 570-586.
5. Brand, A.; Singer, K.; Koehl, G. E.; Kolitzus, M.; Schoenhammer, G.; Thiel, A.; Matos, C.; Bruss, C.; Klobuch, S.; Peter, K., LDHA-associated lactic acid production blunts tumor immunosurveillance by T and NK cells. *Cell metabolism* **2016,** *24* (5), 657-671.
6. Kubinyi, H., Drug research: myths, hype and reality. *Nature Reviews Drug Discovery* **2003,** *2* (8), 665-668.
7. Cook, D.; Brown, D.; Alexander, R.; March, R.; Morgan, P.; Satterthwaite, G.; Pangalos, M. N., Lessons learned from the fate of AstraZeneca's drug pipeline: a five-dimensional framework. *Nature reviews. Drug discovery* **2014,** *13* (6), 419-31.
8. Schuster, D.; Laggner, C.; Langer, T., Why drugs fail-a study on side effects in new chemical entities. *Current pharmaceutical design* **2005,** *11* (27), 3545-3559.
9. Robb, G. R.; McKerrecher, D.; Newcombe, N. J.; Waring, M. J., A chemistry wiki to facilitate and enhance compound design in drug discovery. *Drug Discov Today* **2013,** *18* (3-4), 141-7.
10. Swales, J. G.; Wilkinson, G.; Gallagher, R.; Hammond, C.; O'Donnell, C.; Peter, R., Open access liquid chromatography/tandem mass spectrometry: Implementation of a fully quantitative system in a drug discovery laboratory. *Int J High Through Screen* **2010,** *1*, 1-14.
11. Coe, R., Quantitative whole-body autoradiography. *Regulatory Toxicology and Pharmacology* **2000,** *31* (2), S1-S3.
12. Rönquist-Nii, Y.; Edlund, P. O., Determination of corticosteroids in tissue samples by liquid chromatography–tandem mass spectrometry. *Journal of pharmaceutical and biomedical analysis* **2005,** *37* (2), 341-350.
13. Swales, J. G.; Tucker, J. W.; Strittmatter, N.; Nilsson, A.; Cobice, D.; Clench, M. R.; Mackay, C. L.; Andren, P. E.; Takats, Z.; Webborn, P. J.; Goodwin, R. J., Mass spectrometry imaging of cassette-dosed drugs for higher throughput pharmacokinetic and biodistribution analysis. *Analytical chemistry* **2014,** *86* (16), 8473-80.
14. Manicke, N. E.; Nefliu, M.; Wu, C.; Woods, J. W.; Reiser, V.; Hendrickson, R. C.; Cooks, R. G., Imaging of Lipids in Atheroma by Desorption Electrospray Ionization Mass Spectrometry. *Analytical chemistry* **2009,** *81* (21), 8702-8707.
15. van Remoortere, A.; van Zeijl, R. J.; van den Oever, N.; Franck, J.; Longuespee, R.; Wisztorski, M.; Salzet, M.; Deelder, A. M.; Fournier, I.; McDonnell, L. A., MALDI imaging and profiling MS of higher mass proteins from tissue. *J Am Soc Mass Spectrom* **2010,** *21* (11), 1922-9.
16. Beine, B.; Diehl, H. C.; Meyer, H. E.; Henkel, C., Tissue MALDI Mass Spectrometry Imaging (MALDI MSI) of Peptides. In *Proteomics in Systems Biology: Methods and Protocols*, Reinders, J., Ed. Springer New York: New York, NY, 2016; pp 129-150.
17. Ashton, S.; Song, Y. H.; Nolan, J.; Cadogan, E.; Murray, J.; Odedra, R.; Foster, J.; Hall, P. A.; Low, S.; Taylor, P.; Ellston, R.; Polanska, U. M.; Wilson, J.; Howes, C.; Smith, A.; Goodwin, R. J.; Swales, J. G.; Strittmatter, N.; Takats, Z.; Nilsson, A.; Andren, P.; Trueman, D.; Walker, M.; Reimer, C. L.; Troiano, G.; Parsons, D.; De Witt, D.; Ashford, M.; Hrkach, J.; Zale, S.; Jewsbury, P. J.; Barry, S. T., Aurora kinase inhibitor nanoparticles target tumors with favorable therapeutic index in vivo. *Sci Transl Med* **2016,** *8* (325), 325ra17.
18. Reyzer, M. L.; Hsieh, Y.; Ng, K.; Korfmacher, W. A.; Caprioli, R. M., Direct analysis of drug candidates in tissue by matrix-assisted laser desorption/ionization mass spectrometry. *Journal of mass spectrometry : JMS* **2003,** *38* (10), 1081-92.

19. Takats, Z.; Wiseman, J. M.; Gologan, B.; Cooks, R. G., Mass spectrometry sampling under ambient conditions with desorption electrospray ionization. *Science* **2004,** *306* (5695), 471-3.
20. Eikel, D.; Vavrek, M.; Smith, S.; Bason, C.; Yeh, S.; Korfmacher, W. A.; Henion, J. D., Liquid extraction surface analysis mass spectrometry (LESA-MS) as a novel profiling tool for drug distribution and metabolism analysis: the terfenadine example. *Rapid Commun Mass Spec. 25* (23), 3587-3596.
21. Goodwin, R. J. A.; Nilsson, A.; Mackay, C. L.; Swales, J. G.; Johansson, M. K.; Billger, M.; Andrén, P. E.; Iverson, S. L., Exemplifying the Screening Power of Mass Spectrometry Imaging over Label-Based Technologies for Simultaneous Monitoring of Drug and Metabolite Distributions in Tissue Sections. *Journal of Biomolecular Screening* **2016,** *21* (2), 187-193.
22. Munteanu, B.; Meyer, B.; von Reitzenstein, C.; Burgermeister, E.; Bog, S.; Pahl, A.; Ebert, M. P.; Hopf, C., Label-free in situ monitoring of histone deacetylase drug target engagement by matrix-assisted laser desorption ionization-mass spectrometry biotyping and imaging. *Analytical chemistry* **2014,** *86* (10), 4642-7.
23. Nilsson, A.; Goodwin, R. J.; Swales, J. G.; Gallagher, R.; Shankaran, H.; Sathe, A.; Pradeepan, S.; Xue, A.; Keirstead, N.; Sasaki, J. C.; Andren, P. E.; Gupta, A., Investigating nephrotoxicity of polymyxin derivatives by mapping renal distribution using mass spectrometry imaging. *Chemical research in toxicology* **2015,** *28* (9), 1823-30.
24. Cobice, D. F.; Goodwin, R. J. A.; Andren, P. E.; Nilsson, A.; Mackay, C. L.; Andrew, R., Future technology insight: mass spectrometry imaging as a tool in drug research and development. *British Journal of Pharmacology* **2015,** *172* (13), 3266-3283.
25. Dekker, T. J.; Jones, E. A.; Corver, W. E.; van Zeijl, R. J.; Deelder, A. M.; Tollenaar, R. A.; Mesker, W. E.; Morreau, H.; McDonnell, L. A., Towards imaging metabolic pathways in tissues. *Analytical and bioanalytical chemistry* **2015,** *407* (8), 2167-76.
26. Kallback, P.; Shariatgorji, M.; Nilsson, A.; Andren, P. E., Novel mass spectrometry imaging software assisting labeled normalization and quantitation of drugs and neuropeptides directly in tissue sections. *Journal of proteomics* **2012,** *75* (16), 4941-51.
27. Race, A. M.; Palmer, A. D.; Dexter, A.; Steven, R. T.; Styles, I. B.; Bunch, J., SpectralAnalysis: software for the masses. *Analytical Chemistry* **2016,** *88* (19), 9451-9458.
28. Dexter, A.; Race, A.; Styles, I.; Bunch, J., Testing for multivariate normality in mass spectrometry imaging data: A robust statistical approach for clustering evaluation and the generation of synthetic mass spectrometry imaging datasets. *Analytical chemistry* **2016**.

Figure 1: Stability of Lactate, aspartate, glutamate and glutamine in control kidney sections under different conditions. Bar charts show the relative abundance of the amino acids in the renal cortex and medulla under the different storage conditions over time.

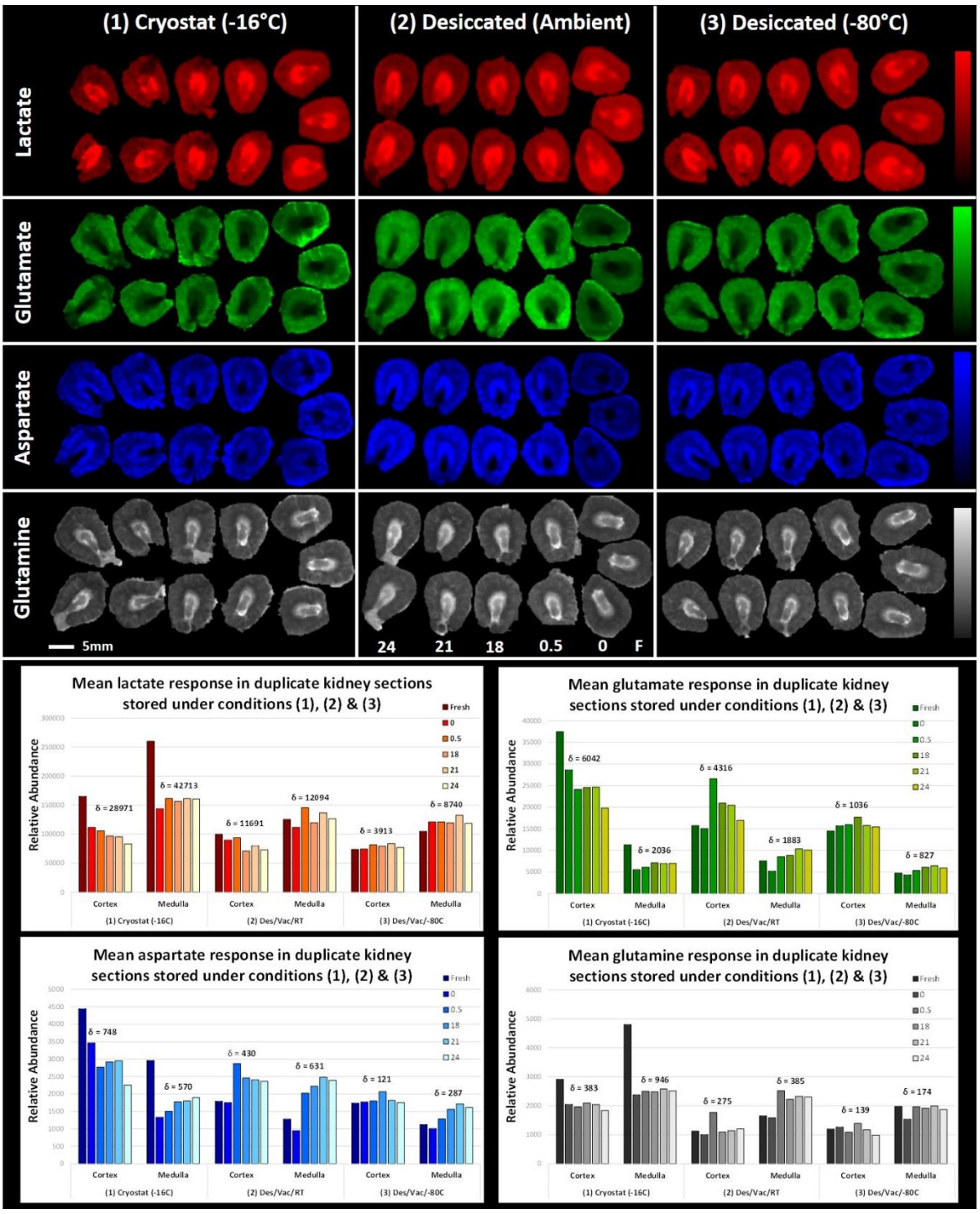

Figure 2: a) Lactate and glutamate distribution in a NCI-H358 tumor model generated using quantitative mass spectrometry imaging. b) A calibration line used generated by spotting $^{13}C3$ stable labelled lactate onto control tissue. c) Graph showing the mean lactate concentration in tumors dosed wiith AZx and vehicle at different timepoints, differentiation between dosed and vehicle treated animals can be seen at the 2 hr timepoint.

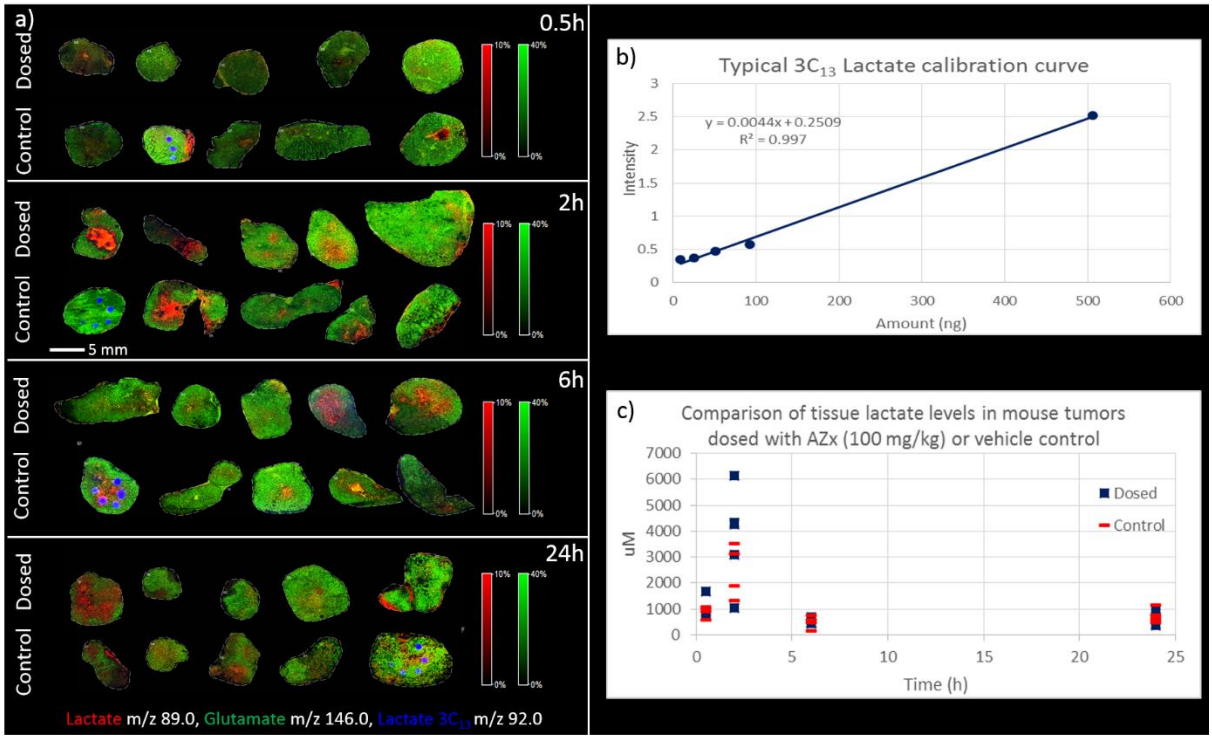

Figure 3: Comparison of four mouse tumor models showing A) lactate (red) and glutamate (green) distribution generated by MALDI-qMSI, B) Clustering images of lactate in the different tumour model tissues and C) Clustering images of glutamate in the different tumour model tissues. The clustering images give a visual representation of the spectrally diverse regions within the tumor tissue. The colors of the different clusters correspond to the colors used in the box plots in figure 4.

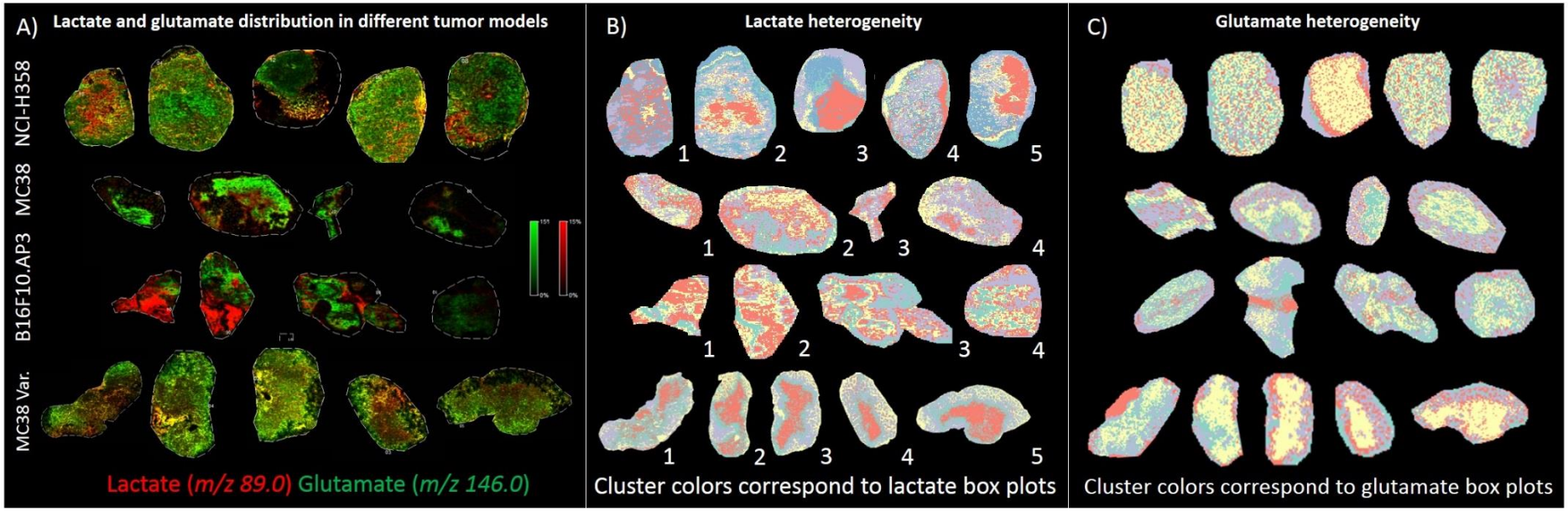

Figure 4: Box plots showing pixel by pixel regio-specific lactate and glutamate concentration. Box colors correspond to the colors used in the clustering images in figure 3B & C.
The boxplots show the differencing heterogeneity of the concentrations of lactate or glutamate based on the different tumour models. The MC38 variant and NCI-H358 tumours have more homogeneously distributed lactate concentration compared to the B15F10 and MC38 models, glutamate concentration is more homogeneous than lactate in all of the models.

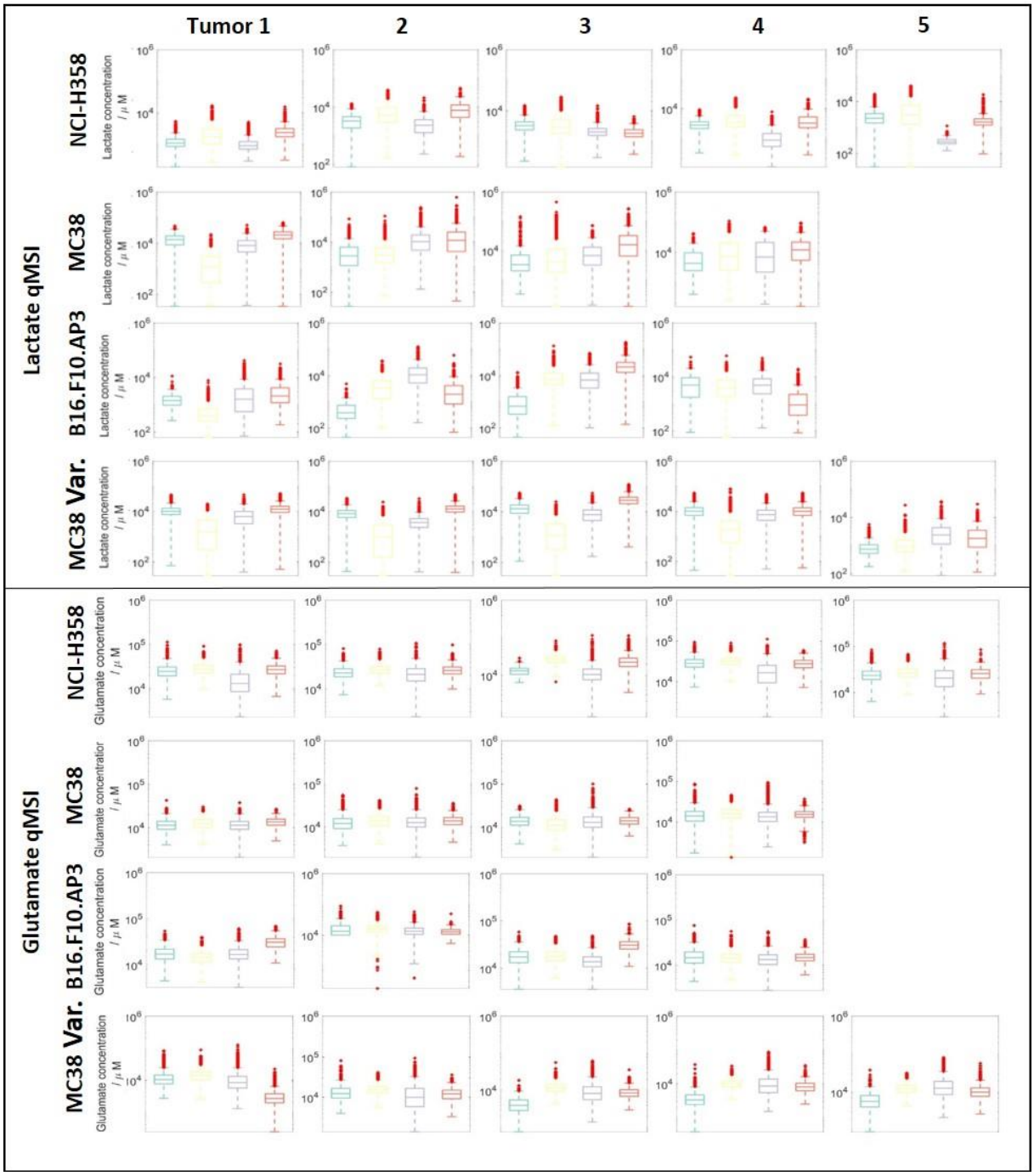

For TOC only

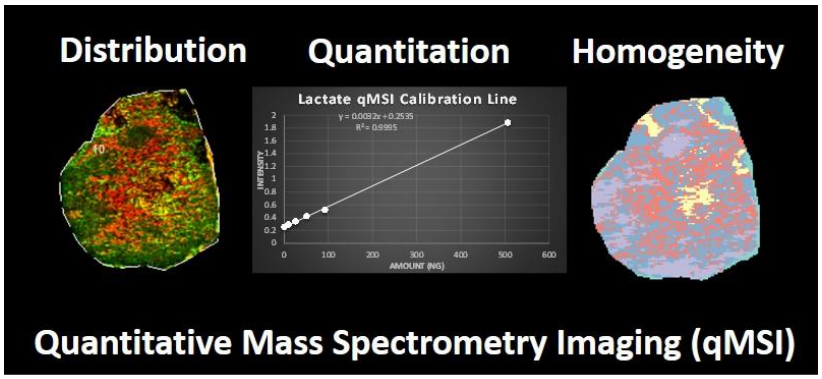
Distribution
Quantitation
Homogeneity
Lactate qMSI Calibration Line
y = 0.0032x + 0.2535
R² = 0.9995
INTENSITY
AMOUNT (NG)
Quantitative Mass Spectrometry Imaging (qMSI)